

2012

DyNi₂Mn—magnetisation and Mössbauer spectroscopy

Jianli Wang

University of Wollongong, jianli@uow.edu.au

Stewart James Campbell

University of New South Wales

Shane Joseph Kennedy

Bragg Institute, ANSTO, Lucas Heights, NSW, Australia

S. X. Dou

University of Wollongong, shi@uow.edu.au

Guang Heng Wu

Chinese Academy Of Sciences

Follow this and additional works at: <https://ro.uow.edu.au/engpapers>



Part of the [Engineering Commons](#)

<https://ro.uow.edu.au/engpapers/4873>

Recommended Citation

Wang, Jianli; Campbell, Stewart James; Kennedy, Shane Joseph; Dou, S. X.; and Wu, Guang Heng:
DyNi₂Mn—magnetisation and Mössbauer spectroscopy 2012, 43-48.
<https://ro.uow.edu.au/engpapers/4873>

DyNi₂Mn – Magnetisation and Mössbauer Spectroscopy

J.L. Wang^{1,2,3}, S.J. Campbell¹, S.J. Kennedy², S.X. Dou³ and G.H. Wu⁴

¹*School of Physical, Environmental and Mathematical Sciences, The University of New South Wales, The Australian Defence Force Academy, Canberra ACT 2600, Australia*

²*Bragg Institute, ANSTO, Lucas Heights, NSW 2234, Australia*

³*Institute for Superconductivity and Electronic Materials, University of Wollongong, Wollongong, NSW 2522, Australia*

⁴*Institute of Physics, Chinese Academy of Science, Beijing 100190, P. R. China*

The physical properties of DyNi₂Mn doped with ⁵⁷Fe have been investigated by X-ray diffraction, magnetisation (10–300 K) and ⁵⁷Fe Mössbauer spectroscopy measurements (5–300 K). DyNi₂Mn(⁵⁷Fe) crystallizes in the MgCu₂-type cubic structure (Fd-3m space group). The ordering temperature is found to be T_C=99(2) K, much higher than those of DyNi₂ (~22 K) and DyMn₂ (~35 K). Analyses of isothermal M-H curves and the related Arrott plots confirm that the magnetic phase transition at T_C is second order. The magnetic entropy change around T_C is 4.0 J/kg K for a magnetic field change of 0 T to 5 T. The spectra above T_C exhibit features consistent with quadrupolar effects while below T_C the spectra exhibit magnetic hyperfine splitting. The Debye temperature for DyNi₂Mn has been determined as θ_D=200(20) K from a fit to the variable temperature isomer shift IS(T).

Key words: Phase transition, Mössbauer spectroscopy, magnetic entropy change

Introduction

RNi₂Mn compounds have been found to exhibit the MgCu₂-type structure even though the ratio of rare earth atoms to transition metal atoms is 1:3 [1-3]. Rietveld refinements of x-ray and neutron diffraction patterns of RNi₂Mn compounds, demonstrated that Mn atoms occupy two inequivalent crystal sites: the 8a and 16d [1, 3, 4]. As part of our systematic investigation of the magnetic properties of this novel RNi₂Mn system, here we present a detailed investigation of the critical magnetic behavior of DyNi₂Mn(⁵⁷Fe) around the magnetic transition temperature by DC magnetisation (10–300 K) and ⁵⁷Fe Mössbauer spectroscopy measurements.

Experimental

An ingot of DyNi₂Mn doped with ~0.5 wt% ⁵⁷Fe, was prepared by standard argon arc-melting the mixtures of starting elements (purities >= 99.9%). X-ray diffraction (Cu-K_α radiation; λ=1.5418 Å) confirmed that DyNi₂Mn(⁵⁷Fe) exhibits the MgCu₂ structure (space group Fd-3m). The lattice constant, a=7.154(3) Å, is slightly larger than that of DyNi₂Mn (a=7.140 Å) reported in [1, 3]; this variation

may be linked with the actual Mn content as discussed in [3]. DC magnetization measurements were carried out over the temperature range 10-340 K in a SQUID magnetometer ($\mu_0 H = 0-5$ T). The ^{57}Fe Mössbauer spectra were obtained between 5 K and 300 K using a standard constant-acceleration spectrometer and a $^{57}\text{CoRh}$ source. The spectrometer was calibrated at room temperature with an α -iron foil.

Results and discussion

The Curie temperature $T_C \sim 99 \pm 2$ K derived from the magnetization data is slightly higher than the published value of $T_C = 94$ K for pure DyNi_2Mn but significantly higher than the values for DyNi_2 ($T_C \sim 22$ K) and DyMn_2 ($T_C \sim 35$ K) [1]. Figs. 1(a) and 1(b) show the M versus H and related Arrott plots of M^2 versus H/M around Curie temperature. The positive slopes of the Arrott plots (Fig. 1(b)) indicate that the phase transition around T_C is second order [3, 5].

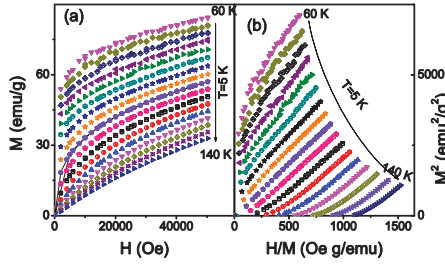


Fig. 1 (a) Magnetization as a function of applied DC field ($H = 0-50$ kOe) around T_C . (b) Arrott-plots of M^2 as a function of H/M for the magnetization data of Fig 1(a). The positive slopes indicate that the transition at T_C is second-order.

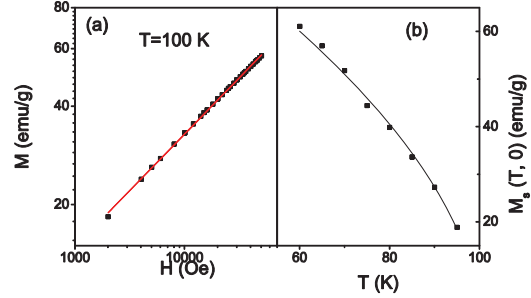


Fig. 2 (a) Critical isotherm at $T = 100$ K on a double-logarithmic scale. The line represents the fit of M vs H resulting in $\delta = 2.90 \pm 0.02$ based on the power relation $M \sim H^{1/\delta}$. (b) Spontaneous magnetization $M_s(T, 0)$ vs T . The line represent the fit of $M_s(T, 0)$ vs T based on equation (1) leading to $T_C = 99.4$ K and $\beta = 0.57 \pm 0.04$.

The critical properties of a second-order magnetic phase transition can be described by critical exponents β , δ and γ derived from magnetization measurements around the transition temperature [e.g. 6]. According to the conventional static scaling law, the exponents can be expressed by the following equations. Below T_C , the temperature dependence of the spontaneous magnetization $M_s(T)$ is governed by the equation:

$$M_s(T) = M_0 |(T - T_C) / T_C|^{-\beta}. \quad (1)$$

The initial susceptibility above T_C is given by

$$\chi_0^{-1}(T) = (h_0 / M_0)(T - T_C / T_C)^\gamma, \quad (2)$$

while at T_C , M and H are related by

$$M = DH^{1/\delta}, \quad (3)$$

where M_0 , h_0/M_0 , and D are the critical amplitudes. As shown in Fig. 2(a), the high-field magnetization data at $T_C = 99(2)$ K, is described well by a straight line of slope $1/\delta$, leading to the fitted value $\delta = 2.90 \pm 0.02$. Following standard procedure,

the limiting $M_S(T, 0)$ values at $H=0$ have been determined from the intercept to the y-axis of Fig. 1(b) by extrapolating the Arrott plots. Fig. 2(b) shows a graph of $M_S(T, 0)$ as a function of T . A fit of the $M_S(T, 0)$ versus T curve to equation (1) results in the value $\beta=0.57\pm 0.04$ (full line in Fig. 2(b)). Applying the Widon scaling relation $\delta = 1 + \gamma/\beta$, to the δ and β values determined above, leads to $\gamma=1.08\pm 0.06$. The mean field interaction model for long range ordering has theoretical critical exponents of $\beta=0.5$, $\gamma=1.0$ and $\delta=3.0$ with theoretical values based on the three dimensional Heisenberg model for short range interactions of $\beta=0.365$, $\gamma=1.386$ and $\delta=4.80$ [7]. The δ , β , γ values derived for $\text{DyNi}_2\text{Mn}({}^{57}\text{Fe})$ indicate that long range interactions dominate the critical behavior around T_C , similar to the behavior detected for TbNi_2Mn [3].

The isothermal entropy change $-\Delta S_M$ associated with a change in magnetic field ΔH from $H = 0$ to value H , has been derived from the Maxwell relation [e.g. 3, 5]

$$\Delta S_M(T, H) = \mu_0 \int_0^H \left(\frac{\partial M}{\partial T} \right)_H dH. \text{ Fig. 3}$$

shows the dependence of the magnetic entropy $-\Delta S_M$ on temperature and external field. The curves exhibit a broad peak around T_C (typical for a second order phase transition [3, 5]) with maximum values around 80 K of $-\Delta S_M \sim 2.52$ J/kg K and 4.0 J/kg K for $\Delta\mu_0 H = 0-3$ T and 0-5 T, respectively. The extended plateau of the $-\Delta S_M$ versus T curve may lead to a large relative cooling power where the RCP is used as an indicator of the cooling efficiency of a magnetocaloric material. For $\text{DyNi}_2\text{Mn}({}^{57}\text{Fe})$, the RCP for the field changes of 0-1 T, 0-2 T, 0-3T, 0-4 T and 0-5 T are 72.6 J/kg, 146.4 J/kg, 169.3 J/kg, 280.2 J/kg and 333.3 J/kg, respectively.

The Mössbauer spectra were analysed as described previously [3, 5] (typical spectra and fits with sub-spectral components are shown in Fig. 4(a)). The 150 K and 300 K spectra exhibit quadrupolar effects consistent with a paramagnetic state as expected above $T_C \sim 100$ K with the 5 K spectrum exhibiting features characteristic of magnetically split sub-spectra consistent with the onset of magnetic hyperfine interactions below T_C . Given that the Mn atoms enter both the 8a and 16d sites in RNi_2Mn compounds [1, 3, 5], it is expected that the dopant

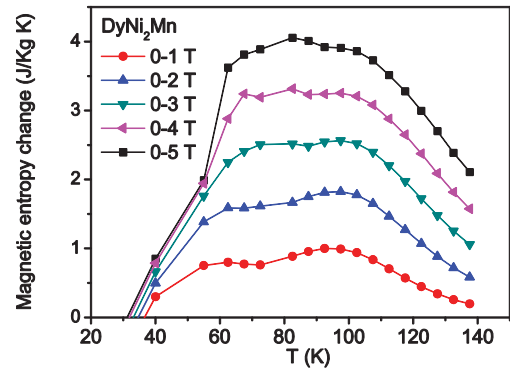


Fig. 3 Temperature dependence of the isothermal magnetic entropy change $-\Delta S_M(T, H)$ as measured in magnetic fields up to 5 T and derived from magnetic data in Fig. 1(a).

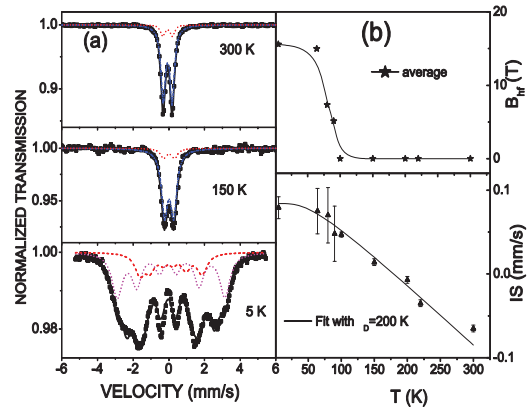


Fig. 4 (a) ${}^{57}\text{Fe}$ Mössbauer spectra of $\text{DyNi}_2\text{Mn}({}^{57}\text{Fe})$ at $T=5$ K, 150 K and 300 K. The fits to the spectra are described in the text [see also 3, 5].

(b) Variation of average magnetic field B_{hf} and isomer shift $IS(T)$ with temperature.

⁵⁷Fe atoms would also enter the 8a and 16d sites. The paramagnetic spectra are described well using two sub-spectra consistent with ⁵⁷Fe atoms located at the 8a and 16d sites. While the spectra for magnetically split spectra would also be expected to be fitted using two sub-sextets to represent ⁵⁷Fe atoms in the 8a and 16d sites, it was found that at least three sub-sextets are needed to provide optimal fits for the spectra below the magnetic ordering temperature T_C [3, 5] (similar behavior has been found for RMn₂ compounds (R=Tb, Dy, Ho) where two sub-spectra rather than a single sub-spectrum are required [8-10]). The observed average hyperfine field values of Fig 4(b) result from contributions to the exchange interactions present in the Dy and transition metal (Ni, Mn) sublattices and correspondingly reflect the magnetic order in the Dy and (Ni, Mn) sublattices.

As shown in Fig. 4(b), the Debye temperature of DyNi₂Mn(⁵⁷Fe) has been determined from the temperature dependence of the isomer shift IS(T) (IS(T)=IS₀(T)+IS_{SODS}(T) [11, 12]). IS₀(T) represents the temperature dependence of the charge density at the probe nucleus which is generally weakly temperature dependent while IS_{SODS}(T), the so-called second-order Doppler shift, can be described in terms of the Debye model for the phonon spectrum by

$$IS_{SODS}(T) = -\frac{3kT}{2mc} \left[\frac{3\theta_D}{8T} + 3\left(\frac{T}{\theta_D}\right)^3 \int_0^\infty \frac{x^3}{e^x - 1} dx \right]$$

(m is the mass of the ⁵⁷Fe nucleus, k

Boltzmann's constant, c the velocity of light, and τ=θ_D/T the reduced temperature). The Debye temperature has been derived to be θ_D = 200±20 K on fitting the mean isomer shift data to the above equation.

References

- 1 J. L. Wang, C. C. Tang, G. H. Wu, Q. L. Liu, N. Tang, W. Q. Wang, W. H. Wang, F. M. Yang, J. K. Liang, F. R. de Boer, and K. H. J. Buschow, *Solid State Commun.* **121**, 615 (2002); J.L. Wang, C. Marquina, M.R. Ibarra and G.H. Wu, *Phys. Rev. B* **73** (2006) 94436;
- 2 D.D. Jackson, S.K. McCall, S.T. Weir, A.B. Karki, D.P. Young, W. Qiu and Y.K. Vohra, *Phys. Rev. B* **75** (2007) 224422
- 3 J.L. Wang, S.J. Campbell, S.J. Kennedy, R. Zeng, S.X. Dou and G.H. Wu, *J Phys.: Condens. Matter.* **23** (2011) 206002
- 4 N. V. Mushnikov, V. S. Gaviko, J. Park, and A. N. Pirogov, *Phys. Rev. B* **79**, 184419 (2009)
- 5 J.L. Wang, S.J. Campbell, R. Zeng, S.X. Dou and S.J. Kennedy, *J Appl. Phys.* **109** (2011) 07E304
- 6 B. Padmanabhan, H. L. Bhat, S. Elizabeth, S. Röbber, U. K. Röbber, K. Dörr, and K. H. Müller, *Phys. Rev. B* **75**, 024419 (2007) and references therein.
- 7 S. N. Kaul, *J. Magn. Magn. Mater.* **53**, 5 (1985).
- 8 J. Marzec, J. Przewoźnik, J. Żukrowski and K. Krop, *J. Magn. Magn. Mater.* **157/158**, 413 (1996).
- 9 P. Stoch, J. Pszczoła, L. Dąbrowski, J. Suwalski and A. Pańta, *J. Alloy. Comp.* **337**, 33 (2002).
- 10 J.L. Oddou, C. Jeandey, R. Ballou, J. Deportes and B. Ouladdiaf, *Solid State Commun.* **85**, 419 (1993).
- 11 G.J. Long, D. Hautot, F. Grandjean, D.T. Morelli and G.P. Meisner, *Phys. Rev. B* **60**, 7410 (1999).
- 12 J. L. Wang, S. J. Campbell, O. Tegus, C. Marquina and M. R. Ibarra, *Phys. Rev. B* **75**, 174423 (2007).